2009

Electrostatic correlations at the Stern layer: Physics or chemistry?

Alex Travesset
Iowa State University, trvsst@ameslab.gov

Electrostatic correlations at the Stern layer: Physics or chemistry?

Abstract
We introduce a minimal free energy describing the interaction of charged groups and counterions including both classical electrostatic and specific interactions. The predictions of the model are compared against the standard model for describing ions next to charged interfaces, consisting of Poisson–Boltzmann theory with additional constants describing ion binding, which are specific to the counterion and the interfacial charge ("chemical binding"). It is shown that the "chemical" model can be appropriately described by an underlying "physical" model over several decades in concentration, but the extracted binding constants are not uniquely defined, as they differ depending on the particular observable quantity being studied. It is also shown that electrostatic correlations for divalent (or higher valence) ions enhance the surface charge by increasing deprotonation, an effect not properly accounted within chemical models. The charged phospholipid phosphatidylserine is analyzed as a concrete example with good agreement with experimental results. We conclude with a detailed discussion on the limitations of chemical or physical models for describing the rich phenomenology of charged interfaces in aqueous media and its relevance to different systems with a particular emphasis on phospholipids.

Keywords
Equilibrium constants, Free energy, Electrostatics, Statistical mechanics models, Protons

Comments
The following article appeared in J. Chem. Phys. 131, 185102 (2009); and may be found at http://dx.doi.org/10.1063/1.3257735.

Electrostatic correlations at the Stern layer: Physics or chemistry?

A. Travesset and S. Vangaveti

Citation: The Journal of Chemical Physics **131**, 185102 (2009); doi: 10.1063/1.3257735
View online: http://dx.doi.org/10.1063/1.3257735
View Table of Contents: http://scitation.aip.org/content/aip/journal/jcp/131/18?ver=pdfcov
Published by the AIP Publishing

Electrostatic correlations at the Stern layer: Physics or chemistry?

A. Travesset[a] and S. Vangaveti
Department of Physics and Astronomy, Iowa State University, Ames, Iowa 50011, USA

(Received 14 August 2009; accepted 10 October 2009; published online 11 November 2009)

We introduce a minimal free energy describing the interaction of charged groups and counterions including both classical electrostatic and specific interactions. The predictions of the model are compared against the standard model for describing ions next to charged interfaces, consisting of Poisson–Boltzmann theory with additional constants describing ion binding, which are specific to the counterion and the interfacial charge ("chemical binding"). It is shown that the "chemical" model can be appropriately described by an underlying "physical" model over several decades in concentration, but the extracted binding constants are not uniquely defined, as they differ depending on the particular observable quantity being studied. It is also shown that electrostatic correlations for divalent (or higher valence) ions enhance the surface charge by increasing deprotonation, an effect not properly accounted within chemical models. The charged phospholipid phosphatidylserine is analyzed as a concrete example with good agreement with experimental results. We conclude with a detailed discussion on the limitations of chemical or physical models for describing the rich phenomenology of charged interfaces in aqueous media and its relevance to different systems with a particular emphasis on phospholipids. © *2009 American Institute of Physics*.
[doi:10.1063/1.3257735]

I. INTRODUCTION

The standard model for describing charged interfaces in aqueous media discriminates between a Stern layer, where ions bind to interfacial groups, and a diffuse layer, where ions are distributed over a characteristic distance before attaining bulk values. While the diffuse layer is universally described by Poisson–Boltzmann (PB) theory[1] (or by more sophisticated theories for higher electrolyte concentrations[2–4]), the description of the Stern layer, on the other hand, resorts to more phenomenological models. A common approach has been to describe ion binding and release as a chemical reaction with some characteristic binding constants,[1,5,6] which are attributed to specific chemical interactions and are assumed to be beyond the scope of classical statistical mechanics. Most commonly, the binding constants are extracted by directly fitting the experimental data. This approach has been extremely successful in describing many experiments, such as, for example, the electrostatic properties of phospholipid systems.[7] Yet, electrostatic interactions are the quintessential example of long-range interactions and binding constants appropriately describe short-range interactions only, thus raising an obvious question about the actual meaning of such binding constants. In addition, at a more practical level, in molecules with many different charged groups it is not generally possible to perform a sufficient number of independent experiments to unambiguously determine all the necessary binding constants.

Over the past years, different approaches treating Stern and diffuse layers entirely within the context of classical statistical mechanics have been proposed.[8–11] In this way, as noted by Lyklema,[12,13] the community investigating aqueous electrolytes has branched out into two, almost completely independent communities, one that uses the standard "chemical" model and its variations, and another embracing the "physical" approach. Despite some notable successes from physical models (see, for example, Refs. 14–16), the bulk of experimental data remains most commonly described by resorting to chemical models.

There are definite examples of chemical interactions at the Stern layer, the most relevant is probably proton release and binding, the mechanism by which acids or bases become charged in aqueous solution. A complete description of the proton is beyond the scope of classical statistical mechanics, so any theory that accounts for proton release and binding must include a parameter (such as the pK_a), which can only be computed from a full quantum chemistry calculation. Yet, when it comes to ions with the electronic structure of a noble gas (such as Na^+, Cs^+, Ca^{2+}, etc.) it should be expected that in most cases, a classical electrostatics description would suffice, and that the chemical binding constants extracted from experiments provide an effective description that can be superseded by an appropriate classical statistical mechanical calculation.

The main motivation for this paper grew from the need to provide a physical model that describes the electrostatic properties of amphiphilic models, particularly phospholipids such as phosphatidic acid (PA) and phosphatidil-inositol-bisphosphate (PIP_2) among others, which participate in almost all signaling pathways across the cell membrane by exquisitely exploiting its electrostatic properties.[17–19] Because these phospholipids include many different charged groups, the description of their electrostatic properties based on the standard chemical approach is far more complex than the one needed for zwitterionic phospholipids such as phos-

[a]Electronic mail: trvsst@ameslab.gov.

phatidylcholine (PC) or phosphatidylethanolamine or singly charged ones such as phosphatidylserine (PS). The focus of this paper will be on presenting the general framework of the model, leaving the detailed predictions and modifications needed to describe signaling phospholipids for a subsequent publication.

Despite the somewhat focused motivation for this paper, the model and results presented find a general applicability to a broad range of systems, extending beyond phospholipids or amphiphilic systems. The paper aims to bridge the gap between physical and chemical descriptions. This is a recent trend in the research in this area; In Ref. 20 it was shown that the concept of Bjerrum pairing, suitably generalized for charged interfaces, provides a convenient way to estimate binding constants from a purely physical model in reasonable agreement with experiments. Reference 21 presents sophisticated Monte Carlo simulations that account for pH variations thus allowing the description of experimental results without resorting to additional parameters. Other groups have systematically accounted for precise mobility measurements by using Monte Carlo or integral equation methods without additional assumptions[22] and a considerable effort has been devoted to combine chemical and physical effects in the field of polyelectrolytes.[23–26]

The critical element in this paper is the role of interfacial charges. This has been a recurrent topic in the statistical mechanics of interfaces. Already in the 1970s, Nelson and McQuarrie[27] solved the PB equation for discrete charges, but experiments[28] failed to validate their findings. More recent treatments[29–32] have revisited the problem, finding that discrete charges add to relatively minor corrections to an approximation where the interface is treated as a smooth background. The crucial aspect between the interaction of interfacial charges and ions is that it describes a strong correlation[20] (see also Ref. 33), which cannot be described as a perturbation from the uniform case. Recent numerical simulations by Madurga *et al.*[34] have clearly shown that distributions of ions in the diffuse layer are greatly affected by the discrete nature of interfacial charges if those are sufficiently exposed to the aqueous solution.

II. MODEL

A. The model

The system consists of a monolayer (with molecular area A_c) of amphiphilic molecules (ALs) forming a charged interface. ALs are acidic or basic and its charge is regulated by its pK_a value. The monolayer is in contact with an aqueous solution of fixed pH containing counterions and coions of general valences. The model we consider builds on three assumptions (see Fig. 1).

(1) Electrostatic correlations are relevant only within the Stern layer.
(2) Counterions and coions within the diffuse layer are weakly correlated and are therefore described by PB theory.
(3) Nonidealities associated with mixing entropies of different species are ignored.

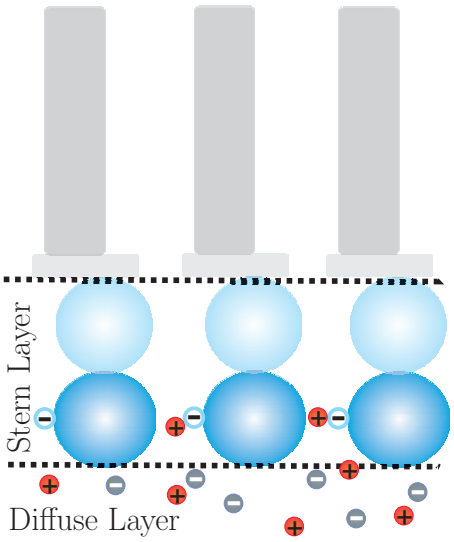

FIG. 1. Schematic representation of a charged system with a distinction between Stern and Diffuse layer.

The justification for assumptions 1 and 2 will be elaborated further below. The last assumption, which is common in most theoretical treatments, will not be discussed any further. It is expected to induce small quantitative errors that can be corrected by introducing additional parameters into the model.

The free energy (F_S) of the system consists of four contributions

$$F_S = F_{\text{Diff}} + F_{\text{Prot}} + F_{\text{Mix}} + F_{\text{Corr}}, \tag{1}$$

where the first term is the free energy associated with building the diffuse layer of counterions, the second term is the free energy associated with proton binding and release, the third term is the entropy of mixing the different species within the monolayer and the last term accounts for the free energy associated with electrostatic correlations. In this paper, only the case of a single pK_a will be considered. The AL head group can be either neutral or charged, according to

$$\text{AL}^- + \text{H}^+ \rightarrow (\text{AL})\text{H}, \tag{2}$$

$$\text{AL}^- + c^q \rightarrow (\text{AL})c^q. \tag{3}$$

The first reaction involves proton release and binding and it is a chemical reaction with an equilibrium constant that is the natural exponential of the pK_a value (in molar units). The second process is a physical process that accounts for ion binding and involves many body effects not entirely describable by a binding constant, as elaborated further below.

The fraction of deprotonated ALs is defined as

$$f_{\text{AL}} = ([\text{AL}^- c^q] + [\text{AL}^-])/([\text{AL}^- c^q] + [\text{AL}^-] + [(\text{AL})\text{H}]), \tag{4}$$

while the fraction of head groups with bound counterions is

$$f_b^{(q)} = [\text{AL}^- c^q]/([\text{AL}^- c^q] + [\text{AL}^-] + [(\text{AL})\text{H}]), \tag{5}$$

where $[\cdots]$ denotes concentration (in molar units). Unless there is ambiguity, the superindex q will be dropped from f_b.

TABLE I. Coefficients for the electrostatic correlation energy [see Eq. (B7)], computed as described in the text for different counterion valences (q). The top value is computed for a triangular lattice, while the bottom one is for the square.

	A_c=70 Å^2			A_c=40 Å^2		
q_{AL}=−1	Mono	Div	Tri	Mono	Div	Tri
a_0	2.107	2.107	2.107	2.107	2.107	2.107
	1.950	1.950	1.950	1.950	1.950	1.950
a_1	0.116	1.635	4.760	0	0.475	2.975
	0.130	1.298	4.924	0	0.589	3.540
a_2	1.268	5.346	12.03	0.834	5.406	12.166
	1.196	5.096	10.60	0.864	4.882	10.600

By definition $f_b < f_{AL}$, as only deprotonated AL are assumed to bind counterions.

It is convenient to introduce the parameter b^0

$$b^0 = \lambda_D/\lambda_G^0, \quad \text{where} \quad \lambda_G^0 = \frac{A_c}{2\pi q l_B}, \tag{6}$$

with λ_D and l_B being the Debye and Bjerrum lengths and q the counterion valence.

The free energy associated with the diffuse layer F_{diff} is given by PB theory (assumption 2). The surface charge includes deprotonated ALs and counterions bound to the head group

$$\frac{F_{Diff}}{N_{AL}k_BT} = |f_{AL} - qf_b|\mathcal{F}_{PB}(b^0(f_{AL} - qf_b)), \tag{7}$$

where N_{AL} is the total number of ALs at the interface and $\mathcal{F}_{PB}$ is the PB free energy. For example, $\mathcal{F}_{PB}(x) = 2(\log(x + \sqrt{x^2+1}) + (1 - \sqrt{1+x^2})/x)$ for both monovalent counterions and coions. For other valences it is not possible to express $\mathcal{F}_{PB}$ in closed analytical form, but it is not difficult to compute numerically (see Appendix A). We recall that if $f_{AL} < qf_b$, the originally negative interface becomes positively charged, an effect that is known as charge inversion or charge reversal.[12,13]

The free energy expression (F_{Prot}) describing proton release and binding is given by

$$\frac{F_{Prot}}{N_{AL}k_BT} = f_{AL}(\mathrm{pK}_a - \mathrm{pH})\log(10), \tag{8}$$

and is derived in detail in Appendix B.

The free energy (F_{Mix}) associated with mixing the different interfacial species is

$$\frac{F_{Mix}}{N_{AL}k_BT} = f_b \log(f_b) + (f_{AL} - f_b)\log(f_{AL} - f_b) + (1 - f_{AL})\log(1 - f_{AL}). \tag{9}$$

The only term left is the one describing electrostatic correlations (F_{Corr}) within the Stern layer. The basic strategy is to account for static correlations as if the system were frozen on a given configuration, and account for thermal fluctuations as perturbations to this configuration. The free energy is

$$\frac{F_{Corr}}{N_{AL}k_BT} = \mathcal{F}_{Corr}(f_{AL}, f_b) - f_b \log(v_0[c]) + \mathcal{F}_{bound}(f_b), \tag{10}$$

here $\mathcal{F}_{Corr}$ encodes the electrostatic correlations of the static system and is computed as a Madelung energy by placing both AL charges and bound ions on either a triangular or a square lattice. Differences in free energies between square or triangular lattices are much smaller than other approximations made, so either case provides equally acceptable results. The term $\mathcal{F}_{Corr}$ accounts for the many body effects that arise from the long-range nature of electrostatic interactions, and it reduces to the leading term of the free energy of a one component plasma[35] if the interface is approximated as a uniform charge. Further details are discussed in Appendix B. Despite the calculation placing the charges in a two-dimensional crystalline state, the expression is assumed to describe the liquid state also. Justification is provided in the context of the one component plasma.[35]

The second term is the favorable entropy of releasing counterions into the bulk solution and the last term $\mathcal{F}_v$ is the thermal free energy associated with counterions bound to the head group. The difference between the last two terms is basically the entropy loss of counterions upon binding. We recall that v_0 defines an arbitrary reference volume, so only the sum of the last two terms defines a term free from arbitrary quantities. The final expression, whose detailed derivation is given in Appendix B, is

$$\frac{F_{Corr}}{N_{AL}k_BT} = -f_{AL}^{3/2}\gamma(f_b)\frac{l_B}{a_L} - f_b \log\left(2\pi r_0^3[c]\sqrt{\frac{11 l_B|q|}{2\pi r_0}}\right). \tag{11}$$

The quantity r_0 is the equilibrium separation between counterion and AL charges, a_L is the average distance between nearest neighbor ALs and $\gamma(f_b)$ is a function that encodes electrostatic correlations and whose explicit expression for the relevant cases discussed in this paper is given in Eq. (B7) and Table I.

Generalization to systems with both monovalent and divalent salts is straightforward, except for the γ-function in $\mathcal{F}_{Corr}$, which requires a minor adjustment, discussed in Appendix B, see Eq. (B8).

B. Free energy minimization

The quantities f_{AL} as well as the different $f_b^{(q)}$ are the main observables to be computed. They are obtained by minimizing the free energy Eq. (1). Both f_{AL} and $f_b^{(q)}$ are not only measurable quantities but completely determine other measurable quantities, such as the ζ-potential. For future reference, we quote the equation determining the minimum of the free energy (particularized for a single counterion specie of valence q)

$$f_{\mathrm{AL}}=\frac{1+K_m[c^q]\exp\left(-\frac{qe\psi(0)}{k_BT}\right)\exp\left(\frac{\partial\mathcal{F}_{\mathrm{Corr}}}{\partial f_b^{(q)}}\right)}{1+10^{\mathrm{pK}_a-\mathrm{pH}}\exp\left(-\frac{e\psi(0)}{k_BT}\right)\exp\left(-\frac{\partial\mathcal{F}_{\mathrm{Corr}}}{\partial f_{\mathrm{AL}}}\right)+K_m[c^q]\exp\left(-\frac{qe\psi(0)}{k_BT}\right)\exp\left(\frac{\partial\mathcal{F}_{\mathrm{Corr}}}{\partial f_b^{(q)}}\right)},$$

$$f_b^{(q)}=\frac{K_m[c^q]\exp\left(-\frac{qe\psi(0)}{k_BT}\right)\exp\left(\frac{\partial\mathcal{F}_{\mathrm{Corr}}}{\partial f_b^{(q)}}\right)}{1+10^{\mathrm{pK}_a-\mathrm{pH}}\exp\left(-\frac{e\psi(0)}{k_BT}\right)\exp\left(-\frac{\partial\mathcal{F}_{\mathrm{Corr}}}{\partial f_{\mathrm{AL}}}\right)+K_m[c^q]\exp\left(-\frac{qe\psi(0)}{k_BT}\right)\exp\left(\frac{\partial\mathcal{F}_{\mathrm{Corr}}}{\partial f_b^{(q)}}\right)}, \tag{12}$$

where $\psi(0)$ is the contact potential and $K_m \equiv 2\pi\sqrt{2\pi r_0/11 l_B r_0^3}$. Despite appearances, This equation is quite involved as $\mathcal{F}_{\mathrm{corr}}$ depends both on f_{AL} and $f_b^{(q)}$, and the contact value potential $\phi(0)$ must be obtained self-consistently from the PB equation for a surface charge density $\sigma=-e(f_{\mathrm{AL}}-qf_b^{(q)})/A_c$. In this paper, the minimum solution was obtained by directly minimizing the free energy by using the MATLAB optimization package.

C. The chemical or LPB model

The standard model (or chemical model) will be revisited within the context of the previous formalism. The correlation term Eq. (11) can be rewritten as

$$\frac{F_{\mathrm{Corr}}}{N_{\mathrm{AL}}k_BT}=-f_b\log\left(K_m\exp\left(\frac{f_{\mathrm{AL}}^{3/2}l_B}{f_b a_L}\gamma(f_b)\right)[c]\right)$$
$$\equiv -f_b\log(K_B^{\mathrm{eff}}(f_b,f_{\mathrm{AL}})[c]). \tag{13}$$

The quantity $K_B^{\mathrm{eff}}(f_b,f_{\mathrm{AL}})$ is not a binding constant as it depends on the variables f_b,f_{AL}, as well as surface density. However, if it is replaced by some mean value $K_B^{(q)}$ that interpolates between the range of f_b,f_{AL} appropriate for each system, then the equations that minimize the free energy simplify to

$$f_{\mathrm{AL}}=\frac{1+K_B^{(q)}[c^q]\exp\left(-\frac{qe\psi(0)}{k_BT}\right)}{1+10^{\mathrm{pK}_a-\mathrm{pH}}\exp\left(-\frac{e\psi(0)}{k_BT}\right)+K_B^{(q)}[c^q]\exp\left(-\frac{qe\psi(0)}{k_BT}\right)},$$

$$f_b^{(q)}=\frac{K_B^{(q)}[c^q]\exp\left(-\frac{qe\psi(0)}{k_BT}\right)}{1+10^{\mathrm{pK}_a-\mathrm{pH}}\exp\left(-\frac{e\psi(0)}{k_BT}\right)+K_B^{(q)}[c^q]\exp\left(-\frac{qe\psi(0)}{k_BT}\right)}. \tag{14}$$

These equations define the chemical model, which consists of a Langmuir absorption isotherm (with binding constant $K_B^{(j)}$) coupled to the PB equation and will be referred to as the LPB model herein. In this way, the LPB model, which has been the standard model to analyze experimental results, for example, in phospholipid systems,[36–40] appears as an approximate effective description for the underlying physical model.

III. RESULTS

A preliminary comparison with simulation results on simple models is provided in Appendix C and its implications are further discussed in the conclusions. This section will be entirely focused on comparison with experiments.

A. A note on coarse-graining phospholipid systems

Glycerol based phospholipids contain two hydrophobic acyl chains and a phosphate group attached to its glycerol backbone. The phosphate group is charged and has an additional group attached to it. If the additional group is serine,

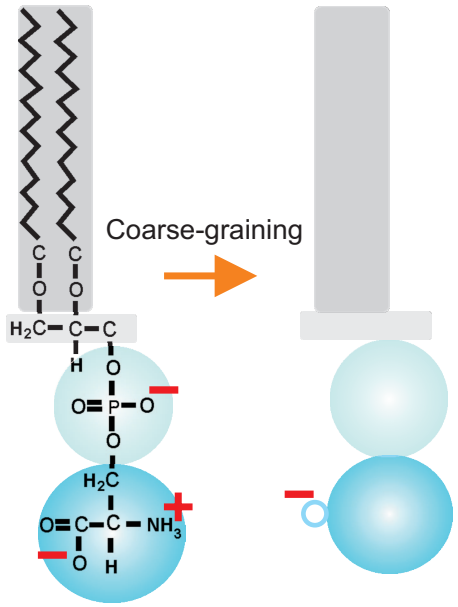

FIG. 2. Schematic representation of the coarse graining of PS.

the phospholipid is PS. It should be noted that there are two acidic (carboxyl and phosphate) and one basic (the amino) groups in PS, see Fig. 2. There are therefore 3 pK_a for PS. The carboxylic and amino groups pK_a have been measured to be 3.6 and 9.8, respectively,[37] while the one in the phosphate group is probably low (1 or less). Thus, at physiological conditions, the overall -1 charge of PS results from two negative and one positive charges. In this paper, the overall PS will be coarse-grained as a -1 charge with $pK_a=3.6$, as shown in Fig. 2. This approximation has been adopted in all descriptions of experimental data and its limitations are further discussed in the conclusions.

B. PS as an example

Unless specified otherwise, it will be assumed that the area per molecule is $A_c \approx 70$ Å^2 and the equilibrium counterion PS-head group distance $r_0=2.8$ Å [see Eq. (11) and Table I]. This distance is the minimum separation between an oxygen atom (~ 1.4 Å) and a counterion such as K^+. These distances correspond to crystallographic radius, as both MD simulations[41–43] and experimental results[44] show that counterions dehydrate upon binding.

Figure 3 shows f_{AL} and f_b for PS in contact with a monovalent salt solution at neutral pH. PS becomes fully deprotonated at about $10^{-3}M$ and at this point about 40% of the PS head groups bind counterions. An attempt to fit the theoretical results within LPB (see Sec. II C) shows that the binding constant extracted from Fig. 3 depends on the particular quantity that is analyzed. If the degree of deprotonation is the quantity of interest, the value $K_B^{(1)}=0.75M^{-1}$ is obtained. If, on the other hand, the amount of ionic binding is what is measured, the value is sensibly smaller $K_B^{(1)}=0.1M^{-1}$, while a ζ-potential would measure a combination of the two quantities and hence, an intermediate value for the binding constant. Experimentally determined values are within the range $(K_B^{(1)}=0.1-1.0)$,[28,36,37,39] and we interpret this dispersion as reflecting the approximate validity of LPB.

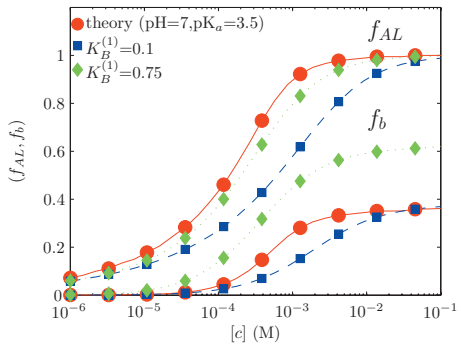

FIG. 3. Plot of f_{AL} and f_b as a function of concentration at neutral pH. The result of the theory is compared with the predictions of LPB with two different binding constants.

More concretely, this dispersion reflects the inherent inaccuracy of describing the Stern layer with short-range forces only.

We can estimate the range of expected values for the binding constants that would be extracted from an experiment by analyzing the minimum free energy equations Eq. (12). For fully deprotonated PS with f_b ranging between 0.1 and 1 (as a significant amount of binding is required) at the molecular area $A_c=70$ Å^2 it is

$$K_B^{(1)} \approx K_m \exp((a_1 + 2f_b a_2)) \sim (0.08 - 0.5)M^{-1}, \qquad (15)$$

where a_1, a_2 are defined in Eq. (B7) and explicit values are given in Table I. Reported binding constants for ions such as K^+ are within this range, while slightly higher values have been quoted for Na^+. Obvious to say that the previous formula has systematic errors arising from the approximations involved in the free energy, but it is difficult to provide a rigorous estimate of these errors.

Divalent counterions at neutral pH fully deprotonate PS ($f_{\mathrm{AL}}=1$), even at trace concentrations $<10^{-6}M$ with a Stern layer that basically neutralizes all the PS charges ($f_b \sim 0.5$), as clear from Fig. 4. In these situations, where f_b varies over such a narrow range, the present model is completely equivalent to LPB with the binding constant obtained from Eq. (13)

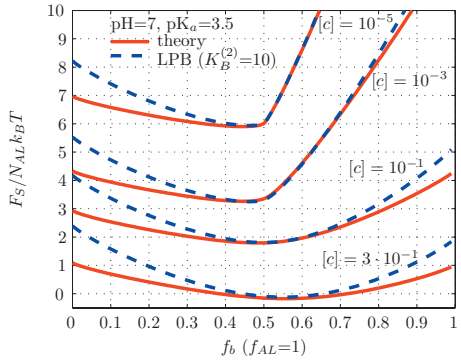

FIG. 4. Free energy as a function of f_b for $f_{\mathrm{AL}}=1$ at neutral pH. Also plotted are the results of the LPB model with $K_B=10$. For $[c]=0.3M$ $f_c>1/2$ thus showing charge inversion. The free energies have been shifted by a constant for proper comparison.

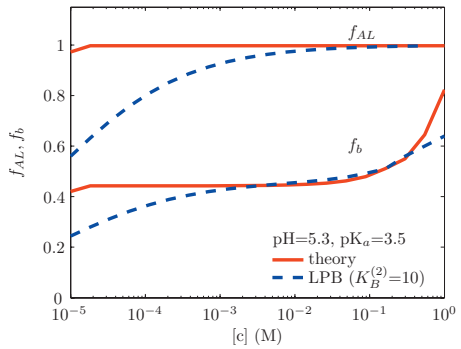

FIG. 5. Plot of f_{AL} and f_b as a function of concentration at pH=5.2. The result of the theory is compared with LPB with K_B=10. The enhanced deprotonation is attributed to long-range electrostatic effects, as discussed in the text.

$$K_B^{(2)} = K_m \exp\left(\frac{l_B}{a_L}(a_1 + a_2)\right) \approx 7M^{-1}, \tag{16}$$

in excellent agreement with experimental results $K_B \sim 10M^{-1}$,[36] as well as with other, less sophisticated theoretical estimates.[20] In Fig. 4 the comparison between the free energy of this model and LPB ($K_B^{(1)}$=10) clearly shows the equivalence between both models. Above $0.1M$ the interface is slightly positively charged, thus exhibiting the phenomenon of charge inversion.[12,33]

In order to provide a better illustration on the effect of divalent ions on PS and the inequivalence of the present model with LPB, results at pH=5.2 are shown in Fig. 5. Here again, the theoretical curve is well described by LPB with $K_B^{(2)}$=10, but only for concentrations $[c] > 10^{-3}$, while at low concentrations LPB predicts a partially protonated PS. Results for lower pH values show more dramatic differences. This figure also illustrates how the free energy gain from electrostatic correlations forces higher deprotonation than predicted by LPB. It is also noticeably that although the onset of charge inversion is the same, its magnitude is enhanced (as compared with LPB) at large concentrations, as correlations grow for increasing f_b.

Figure 6 analyzes a system with both monovalent and divalent salts. The monovalent salt concentration was taken as $[c^{(1)}]=0.1M$, which is the limit of applicability for PB. As divalent salt concentration is increased, divalent ions replace

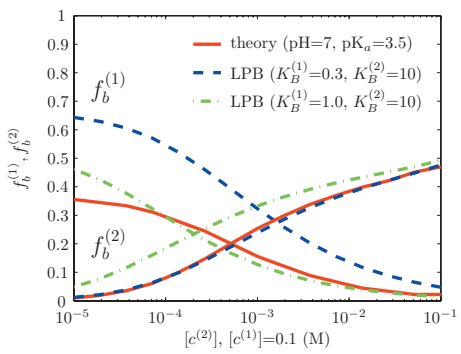

FIG. 6. Plot of f_{AL} and f_b as a function of divalent salt concentration for fixed monovalent concentration $[c^{(1)}]=0.1M$ at neutral pH. The result of the theory is compared with the predictions from LPB with two different values for the binding constants.

the monovalent ones at the Stern layer. It is remarkable that the effect of divalent salt is already significant for $[c^{(2)}] > 10^{-5}M$, four orders of magnitude lower than the monovalent salt concentration in the system. This particular system (PS with divalent ions at fixed [NaCl]=$0.1M$) was extensively studied in Ref. 36. Experiments reported excellent agreement of ζ-potential measurements with LPB ($K_B^{(1)}$=0.6, $K_B^{(2)}$=10). These binding constants are in agreement with the ones predicted by this theory for solutions with only monovalent or divalent salts. A more detailed analysis, shown in Fig. 6 shows that the quantities $f_b^{(1)}$ and $f_b^{(2)}$ are quite sensitive to the value of $K_B^{(1)}$ and in fact $K_B^{(1)} \sim 1$ fits well $f_b^{(1)}$ but shows some slight discrepancy for $f_b^{(2)}$ while $K_B^{(1)} \sim 0.3$ fits $f_b^{(2)}$, but with some discrepancy on $f_b^{(1)}$. If the ζ-potential, which is a combination of $f_b^{(1)}$ and $f_b^{(2)}$, would be fitted instead, another value for $K_B^{(1)}$, intermediate between the two, would be obtained. Although those are not dramatic variations, they do reflect, once again, the limitations of LPB, as previously discussed for monovalent ions.

IV. CONCLUSIONS

A. Summary of results

This paper has presented a minimal model that describes both the Stern and diffuse layer by classical electrostatics, except for protons (hydronium ions), which require the introduction of a chemical binding constant (the pK$_a$). The model leads to a set of equations that can be solved self-consistently by numerical minimization. Despite its relative simplicity, the model successfully describes experimental results on PS without resorting to fitting parameters.

The model compares well with available MD simulation results as shown in Appendix C, thus extending a previous model based on Bjerrum pairing.[20] In particular, the potential of mean force clearly reveals the fundamental role played by discrete interfacial charges as opposed to a smooth charge distribution. A more systematic comparison between theory and MD simulations will be discussed elsewhere.

Our results provide a clear explanation on the success of chemical models to describe experimental data, allows to highlight its limitations and points out effects that cannot accurately be accounted for by those. Measurable quantities computed from the model can be described with reasonable accuracy by the standard chemical model (or LPB, see Sec. III) over several decades in salt concentration. Yet, the actual values of the binding constants extracted by fitting the model by LPB show an inherent dispersion, depending on the particular observable studied. Rather interestingly, this dispersion is within the range of experimentally reported values for binding constants and does reflect the limitations of describing the long-range electrostatic force by binding constants that can only account for short-range interactions.

The effect of long-range electrostatics at the Stern layer becomes more dramatic for ions of higher valency. The enhanced (as compared with monovalent ions) electrostatic correlation free energy makes it more favorable to increase the interfacial charge via deprotonation and replace the Stern layer with divalent (or higher valency) counterions, as shown in Fig. 5. This effect is expected to become more dramatic

for AL with many charged groups and is not accurately described by the LPB model as shown in Fig. 5. The same effect has been theoretically discussed in Ref. 43, and there is experimental evidence on monolayers of PA and PIP_2 at the air-water interface.[44–47]

Despite its limitations, unless high precision data is obtained on a simple system where parameters such as molecular area and charge can be precisely controlled over a wide range of values, chemical models generally provide a reasonably effective description of experimental results.

B. Chemical versus physical effects

Except for the proton, which requires the specification of the pK_a, the remaining ions have been assumed to interact with the charged interface via classical electrostatics. Due to its inherent stability, ions with the electronic structure of a noble gas, such as the alkali (Na^+, K^+, etc.), alkali earth ions (Ca^{2+}, Ba^{2+}, etc.) or Halogens (Cl^-, Br^-, I^-, etc.) are the obvious candidates to be described by classical electrostatics, while other soluble ions such as transition metals (Cu^{2+}, Pb^{2+}, Cd^{2+}, Ni^{2+}, Fe^{2+}, etc.) are likely to exhibit some degree of covalent bonding with most interfacial groups.

Some support for this hypothesis can be given by the analysis of stability constants,[48] which account for the binding constants of ions to certain ligands. Sticking to the example of carboxylic groups, a look at the entries for simple carboxylic acids (formic, acetic, and propanoic), shows binding constants within the range (with some dispersion) $K_B^{(1)} \sim 0.5$, $K_B^{(2)} \sim 10M^{-1}$, the typical values obtained from our model, and thus supporting the idea of a classical electrostatic interaction between those ions and carboxylic groups. Entries for the transition metal ions, however, are between 5 to 10 times larger, thus providing strong evidence for some degree of covalency or chemical specificity. Even for ions such as Ca^{2+} the situation is not as simple; the entry for Carbonic acid with Ca^{2+} shows four entries, the first two correspond to binding to $CaCO_3^{2-}$ and $CaCO_3H^-$ and have values $K_{B,2}^2=1400$ and $K_B^2=10.0$, while the two additional entries are solubility products (calcite and aragonite crystals) with $CaCO_3^{2-}$, thus showing that besides the classical electrostatic interactions corresponding to the first two entries (see Refs. 20 and 49 for the first, which corresponds to Bjerrum pairing), Ca^{2+} ions show some degree of covalent interaction, depending on the ligand. Similar conclusions are reached by analyzing phosphate, amino or any other groups.

Another source for specific ionic effects is related to explicit solvent effects. Ions have hydration sheaths, and those are distorted or eliminated upon binding. Generally, it should not be a dominant effect as most commonly, cations bind to interfacial oxygens, so upon binding, they trade one oxygen (from the water molecule at its hydration sheath) to another with basically no change in enthalpy, and if anything, a gain in entropy for the water molecules that leave the hydration sheath. Yet, even for those cases where these free energies need to be included, the dehydration involves short-range interactions and therefore, there are describable by binding constants, which can be computed, for example, from more detailed atomistic simulations.

A general model applicable to all situations requires the inclusion of specific interactions related to the ions and the charged or uncharged groups at the interface. The critical quantity that needs to be known is the ionic-specific free energy ΔG_{Spec}, defined as the free energy gain once the universal electrostatic interaction has been subtracted. Once this quantity is known, an unambiguous binding constant can be defined and a term such as Eq. (14) is added in addition to the free energy Eq. (1). The next issue is how to determine ΔG_{Spec}. A rough estimate is probably obtained by subtracting from the binding free energy the reference free energy of an interfacial-counterion pair, which can be calculated within the present theory. For example, taking $10M^{-1}$ as the reference binding constant for a purely electrostatic interaction, and given that $K_B^{(2)}=40M^{-1}$ for binding of Ni^{2+} to PS^-, this gives $\Delta G_{\mathrm{Spec}}^{\mathrm{PS}}=-3.40k_BT$ for PS^{-1}-Ni^{2+}. Of course this number is specific for that particular system. First principle calculations, without resorting to experimental data, would certainly require sophisticated quantum chemistry calculations.

C. Implications for phospholipid systems

Concrete application to a simple coarse-grained model of PS shows good agreement with experimental results,[36] despite the questionable approximation of modeling PS as consisting of a single negative charge, as discussed in Sec. III A. The large values of ion binding constants in zwitterionic phospholipids such as PC (Ref. 36) ($\sim 3M^{-1}$) show that the positively charged amino group is sufficiently far apart to preempt the negatively charged oxygen within the phosphate group to bind counterions, which could be relevant for PS also. These considerations demand a more detailed modeling of the phospholipid head group, where all charges are included. In fact, Ref. 36 reports that the binding constant for Ca^{2+} with PS is enhanced by a factor of almost 3 at low monovalent salt concentration, a result that is not reproduced by our model (data not shown). This is a large enhancement, not observed in other molecules for decreasing ionic strength,[48] but a more detailed analysis is needed. These considerations become even more relevant for investigating complex phospholipids such as PA (Ref. 44) or PIP_2.[40] It is not difficult to incorporate the nuances required to describe those phospholipids, and they will be fully addressed in a subsequent publication. Those effects are key for a proper understanding of electrostatic induced phase separation in lipid mixtures, as discussed, for example, in Ref. 50.

D. Outlook

As for the question posed in the title of this paper on whether electrostatic correlations near charged interfaces are described by physics (universal) or chemistry (specific), the answer seems clear: any model that aims to be complete and realistic must incorporate both.

ACKNOWLEDGMENTS

A.T. acknowledges endless discussions with J. Faraudo and C. Calero and D. Vaknin for his many insightful remarks and inspiring experimental results. This work is supported by NSF CAREER Award No. DMR-0748475.

APPENDIX A: GENERAL EXPRESSION FOR PB WITH BOTH MONOVALENT AND DIVALENT SALTS

Here we just quote the main formulas for the free energy of a planar charged interface in contact with a solution containing both monovalent and divalent salt with respective bulk concentrations $c^{(1)}$ and $c^{(2)}$ within PB. The expression is

$$\frac{\mathcal{F}}{N_B k_B T} \equiv \mathcal{F}_{\rm PB} = \left| \frac{e\psi(0)}{k_B T} \right| - \frac{1}{2b} \mathcal{Y}\left(\frac{e\psi(0)}{k_B T}, \frac{c^{(2)}}{3c^{(2)} + c^{(1)}} \right), \tag{A1}$$

where N_B is the number of charges (of valence -1) at the interface and b has been defined in Eq. (6) (and used here with $q=1$). The Debye length is $\lambda_D = 1/\sqrt{8\pi l_B (3c^{(2)} + c^{(1)})}$ and the function $\mathcal{Y}(x,a)$ is defined as

$$\mathcal{Y}(x,a) \equiv \frac{1-3a}{2\sqrt{2a}} \log\left(\frac{1 - a + 2a\exp(-x) + 2\sqrt{a(1-a)\exp(-x) + a^2\exp(-2x)}}{(1+\sqrt{a})^2} \right) + \frac{a\exp(-2x) + (1+a)\exp(-x) + 2(1-a)}{\sqrt{(1-a)\exp(-x) + a\exp(-2x)}} - 3. \tag{A2}$$

The relation between the surface charge σ and the contact potential $\psi(0)$ is obtained from the PB equation, and can only be solved analytically for the case of monovalent salts. For the other cases it is solved numerically and the result is inserted into Eq. (A1), thus providing the free energy.

APPENDIX B: DERIVATION AND DETAILS OF THE DIFFERENT TERMS FORMING THE FREE ENERGY

1. Derivation of $F_{\rm Prot}$

The free energy of a charged interface consisting of N_B charges is given within PB by

$$\frac{F}{k_B T} = 2N_B(\log(b + \sqrt{b^2+1}) + (1 - \sqrt{1+b^2})/b) + \sum_a N_a(\log(N_a v_0/V) - 1) \equiv \frac{F_E}{k_B T}, \tag{B1}$$

where b is the ratio of the Debye and the Guoy–Chapman length. The last term, which is the same for other counterion and coion valences, is the bulk entropy of the ionic species. Because the interface gets charged by releasing protons, there are $N^1_{\rm prot} = N_B$ protons in bulk whose origin are the interfacial groups, so the last term in Eq. (B1) is dependent on $N^1_{\rm prot}$. It will be assumed that the number of protons in bulk $N^0_{\rm prot}$ largely exceeds the ones released by charging the interface ($N^1_{\rm prot}/N^0_{\rm prot} \ll 1$).

The free energy is computed from a reference state where all the interfacial groups are deprotonated $N_B = N_{\rm AL}$ (or $N_{\rm prot} = N_{\rm AL}$), thus the second term in Eq. (B1) becomes

$$\frac{F_E}{k_B T} = \frac{F_{\rm ref}}{k_B T} + N^1_{\rm prot} \log(N^0_{\rm prot} v_0/V), \tag{B2}$$

where $F_{\rm ref}$ is independent of $N^1_{\rm prot}$. If the reference volume v_0 is taken as $v_0 = 1M$ the previous term becomes $\log(N^0_{\rm prot} v_0/V) \equiv -{\rm pH}\log(10)$.

Generally, protons have a favorable free energy (ε_A) to remain bound to the AL head group. This is taken into account as

$$\frac{F_A}{k_B T} = -\varepsilon_A (N_{\rm AL} - N_B). \tag{B3}$$

The energy ε_A is related to the binding constant K_a between AL groups and protons according to $K_a = 1/v_0 \exp(-\varepsilon_A/k_B T)$. If $v_0 = 1M$, then $pK_a = \log_{10}(K_a)$ and $\varepsilon_A = k_B T \log(10) pK_a$. Consistently using the reference volume $v_0 = 1M$, the two terms (B2) and (B3) become

$$\frac{F_{\rm Prot}}{N_{\rm AL} k_B T} = f_{\rm AL}({\rm pK}_a - {\rm pH})\log(10), \tag{B4}$$

which is the result quoted in Eq. (8).

2. Derivation of $F_{\rm Corr}$ (1 pK_a case)

This term contains three contributions. The first term is the static electrostatic energy, where both interfacial charges and counterions are at fixed positions, and is the equivalent of the Madelung energy for ionic crystals. The remaining two terms have a thermal origin and will be considered further below. The static electrostatic energy is computed by placing the AL charges on a planar lattice. It is assumed that counterions are contained on the same plane defined by the lattice, and that the free energy is expressed as a function of the lattice constant a_L, which is related to the molecular area A_c as $a_L = \sqrt{2A_c/\sqrt{3}}$ (triangular) or $a_L = \sqrt{A_c}$ (square). The free energy is computed from

$$\mathcal{F}_{\rm Corr} = \frac{1}{2}{\sum_{i,j}}' q_i q_j \frac{e^2}{\varepsilon_w r_{ij}}, \tag{B5}$$

where the prime indicates that the term with $i=j$ is not included in the summation. Because this summation runs over the entire lattice, it requires the use of Ewald summation

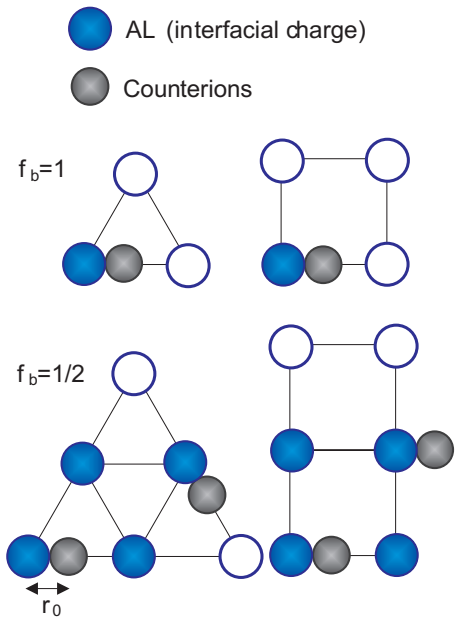

FIG. 7. Configurations used to compute the static correlation energy $f_b=1$ and $f_b=1/2$. The configuration $f_b=1/2$ can be used to compute $f_b^{(1)}$ and $f_b^{(2)}$ by placing a divalent and a monovalent charge on every site. Empty circles do not belong to the unit cell and are obtained from lattice translations.

techniques for systems with two-dimensional periodicity.[51] The result is

$$\frac{\mathcal{F}_{\mathrm{Corr}}}{N_{\mathrm{AL}}k_BT}=-f_{\mathrm{AL}}^{3/2}\gamma(f_b)\frac{l_B}{a_L}, \tag{B6}$$

where $\gamma(f_b)$ is a function of the fraction of counterions bound to the head group f_b. For $f_b=0$, the results are the Madelung energies of a triangular ($\gamma=2.107$) or a square ($\gamma=1.95$) lattice. The sum (B5) is evaluated at two values of f_b ($f_b=1/2$ and $f_b=1$) (see Fig. 7) and the full $\gamma(f_b)$ function is constructed as a polynomial that interpolates among these two values

$$\gamma(f_b)=a_0+a_1f_b+a_2f_b^2. \tag{B7}$$

Evaluation of the Ewald sum for intermediate values of f_b did not show any significant improvement by considering a higher order polynomial or by optimizing its coefficients by a best fit. It should be pointed out that the function $\gamma(f_b)$ involves an approximation, as the coefficients a_i are computed at $f_{\mathrm{AL}}=1$, so the expression for the correlation energy is expected to become somewhat inaccurate for $f_{\mathrm{AL}}\ll 1$.

The function $\gamma(f_b)$ is dependent on the relative position of the counterions with respect to the AL charges. Numerical minimization shows that the minimum electrostatic energy in Eq. (B6) occurs when the counterions are as close as possible to the AL charged groups. The γ-function was therefore computed for given molecular area and typical AL-counterion distance of r_0, as shown in Fig. 7. Reasonable variation on the positions of the counterions typically change Madelung energies by less than 10%. The a_i coefficients for the different cases relevant to this paper are shown in Table I. If both monovalent and divalent ions are involved, the γ-function is dependent on the two variables $f_b^{(1)}$ and $f_b^{(2)}$

$$\gamma(f_b^{(1)},f_b^{(2)})=a_0+a_1^{(1)}f_b^{(1)}+a_1^{(2)}f_b^{(2)}+a_2^{(1)}(f_b^{(1)})^2+a_2^{(2)}(f_b^{(2)})^2+a_2^{(1,2)}f_b^{(1)}f_b^{(2)}, \tag{B8}$$

where only the $a_2^{(1,2)}$ coefficient is unknown as the others have already been determined in Table I. This coefficient was computed by evaluating the Ewald sum for $f_b^{(1)}=1/4$ and $f_b^{(2)}=1/4$ and obtaining the unknown coefficient from Eq. (B8) and the actual results in Table I. The result for a triangular lattice with $A_c=70$ Å^2 and $r_0=2.8$ Å is $a_2^{(1,2)}=4.93$.

Similarly as for protons, counterion binding and release involves changes in bulk entropy. Adapting the same derivation (see Appendix B 1) leads to the second term in F_{Corr}

$$\frac{F}{N_{\mathrm{AL}}k_BT}=-f_b\log(v_0[c]), \tag{B9}$$

where v_0 is an arbitrary volume.

Bound counterions are not immobile, as assumed in the calculation of the first term Eq. (B6), but do fluctuate from their equilibrium positions, and this is the origin of the third contribution to F_{Corr} in Eq. (11). The fluctuation free energy of counterions bound to the head group requires a repulsive short-range potential between counterions and AL charges, which is assumed to be of the form $V(r)=4\epsilon(\sigma/r)^{12}$. It is also assumed that the dominant electric field relevant for counterion fluctuations is the one from its nearest AL charge. In this way, the attractive electrostatic and the repulsive short-range potential lead to an equilibrium distance r_0 with quadratic fluctuations at leading order

$$\delta\mathcal{F}_{\mathrm{Corr}}(r)=\frac{11|q|e^2}{2r_0^3\varepsilon_w}(r-r_0)^2\equiv\frac{\kappa}{2}(r-r_0)^2, \tag{B10}$$

so the fluctuation free energy per particle becomes

$$2\pi\int drr^2\exp\left(-\frac{\kappa(r-r_0)^2}{2k_BT}\right)=\sqrt{\frac{2\pi}{11}}\frac{2\pi r_0^3}{\sqrt{ql_B/r_0}}, \tag{B11}$$

where $\kappa r_0^2/k_BT=11qe^2/K_BTr_0\varepsilon_w=11ql_B/r_0\gg 1$ has been used to simplify the above expression. It is assumed that the AL charge is anchored to the head group and therefore the available solid angle is 2π,[20] as opposed to 4π (if the AL charge was in solution). The free energy is

$$\mathcal{F}_{\mathrm{bound}}=f_b\log\left(\frac{v_0}{2\pi r_0^3}\sqrt{\frac{l_B|q_c|}{r_0}}\sqrt{\frac{11}{2\pi}}\right). \tag{B12}$$

The physical interpretation is that counterions fluctuate over a distance $\sim r_0\sqrt{r_0/l_B|q_C|}$ along the direction of the AL-counterion axis.

The three terms (B7), (B9), and (B12) provide the explicit expressions for the electrostatic correlation free energy Eq. (11).

APPENDIX C: COMPARISON WITH NUMERICAL SIMULATIONS

Recent molecular dynamics (MD) simulations by Calero and Faraudo[52] have explored in detail the role of interfacial charges by performing numerical simulations of an electrolyte primitive model of 2:1 salt near discrete interfacial negative charges on a plane and arranged in a square lattice.

TABLE II. Comparison between the results of simulation (Ref. 52) and the theoretical results for σ at three different 2:1 salt concentrations. The results correspond to a square lattice with $q_{AL}=-1$ interfacial charges with $r_0=3$ Å and bare $\sigma=-0.1$ nm^{-2} ($A_c=1000$ Å^2).

$[c]$ (M)	σ (MD) (nm^{-2})	σ (theor.) (nm^{-2})	Error (%)
0.023	−0.079	−0.074	6
0.033	−0.078	−0.070	10
0.058	−0.074	−0.062	16

Although the paper is mainly focused on high electrolyte concentrations, where the role of electrostatic correlations becomes significant beyond the Stern layer, it is possible to provide some comparison with the present theory. A more systematic comparison will be provided in the future.

We will first consider the density of charge, $\sigma=-e1-2f_b^{(q)}/A_c$ (note that $f_{AL}=1$ and only divalent ions are considered). The comparison MD simulation versus theory for σ, shown in Table II show good agreement for the lowest concentrations and diverge slightly at the largest concentration. Most likely, this divergence is due to the neglect of screening effects at the Stern layer, which would decrease the correlations and with it, the number of counterions bound to head groups. These effects can easily be incorporated into the sum defining the gamma coefficients Eq. (B6). Although relevant for comparing with simulation results, the effect of screening at the Stern layer may not need be included in some experiments. In order to extent the results to even higher concentrations $>0.1M$, activity coefficients that depart from unity need to be considered, a result not included by the present theory, as PB theory is assumed. We point out that it is possible to account for activity coefficients by including Bjerrum pairing in bulk.[53,54]

Another important quantity is the potential of mean force. This quantity elucidates the role of discrete charges and provides a clear insight on the consequences of the present theory. Results for the potential of mean force V_{MF} are shown in Fig. 8 for the same simulations described previously, where it is shown that the potential of mean force has a simple analytical form of the type

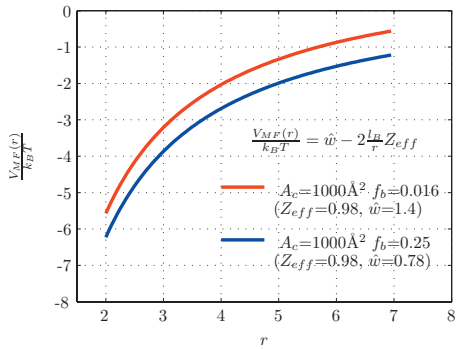

FIG. 8. Plot of the potential of mean force for the same system as in the previous figure. The fits to the potential (C1) are indistinguishable from the theory prediction.

$$\frac{V_{MF}(r)}{k_BT} = \hat{w} - 2\frac{l_B}{r}Z_{eff}, \tag{C1}$$

where Z_{eff} is close but smaller than 1. The second term of the potential (with $Z_{eff}=1$) is the prediction from Bjerrum theory,[20] while $\hat{w}$ encodes additional correlations among counterions as well counterions and interfacial charges. Those predictions are in excellent agreement with the numerical simulations by Calero and Faraudo[52] and clearly show the distinct role played by interfacial charges: In a smooth distribution, the potential of mean force could never display a $1/r$ decay, as its origin is the direct (Bjerrum) interaction between the counterion and the interfacial charge closest to it.

APPENDIX D: CONNECTION WITH BJERRUM PAIRING THEORY

Bjerrum pairing theory[20] is the LPB theory

$$\frac{F_{Corr}}{N_{AL}k_BT} = -f_b \log(K_B v_0[c]), \tag{D1}$$

with the explicit expression for K_B borrowed from Bjerrum pairing theory[49,53]

$$K_B = 2\pi\int_{r_0}^{|q_c l_B|/2} drr^2 \exp\left(q\frac{l_B}{r}\right). \tag{D2}$$

This expression is closely related to the effective K_B^{eff} defined in Eq. (13). This is more clearly seen in the limit $ql_B/r_0 \gg 1$, where the Bjerrum constant above becomes

$$K_B \approx 2\pi\frac{r_0^4}{ql_B}\exp(ql_B/r_0)(1+4r_0/(ql_B)+\cdots). \tag{D3}$$

The term in the exponential is the electrostatic energy when particles are frozen in their positions [Eq. (B6)], while the prefactor contains the free energy of the fluctuations Eq. (B12). Compared with more rigorous expressions such as Eq. (16) the simple expression above does not depend on f_{AL}, f_b, molecular area A_c, etc., but it nevertheless provides a reasonable semiquantitative estimate for binding constants.[20]

Bjerrum pairing assumes a hard core potential and the formulas used in this paper are for softer $1/r^{12}$-potentials, which explains the different analytical prefactors. Finally, the expansion Eq. (D3) is significantly inaccurate for $q_C l_B/r_0 \lesssim 20$ as in that case, fluctuations from r_0 are not small.

[1] J. Lyklema, *Fundamentals of Interface and Colloid Science* (Academic, New York, 1991), Vols. 1-2.
[2] R. Kjellander and J. D. Mitchell, J. Chem. Phys. **101**, 603 (1994).
[3] P. Attard, Phys. Rev. E **48**, 3604 (1993).
[4] M. Lozada-Cassou, in *Fundamentals of Inhomogeneus Fluids*, edited by D. J. Henderson (Dekker, New York, 1992), Chap. 8; E. Gonzalez-Tobar and M. Lozada-Cassou, J. Phys. Chem. **93**, 3761 (1989).
[5] B. W. Ninham and V. A. Parsegian, J. Theor. Biol. **31**, 405 (1971).
[6] T. W. Healy and L. R. White, Adv. Colloid Interface Sci. **9**, 303 (1978).
[7] S. McLaughlin, Annu. Rev. Biophys. Chem. **18**, 113 (1989).
[8] A. Yu. Grosberg, T. T. Nguyen, and B. I. Shklovskii, Rev. Mod. Phys. **74**, 329 (2002).
[9] H. Boroudjerdi, Y.-W. Kim, A. Naji, R. R. Netz, X. Schlagberger, and A. Serr, Phys. Rep. **416**, 129 (2005).
[10] Y. Levin, Rep. Prog. Phys. **65**, 1577 (2002).
[11] R. Messina, J. Phys.: Condens. Matter **21**, 113102 (2009).

[12] J. Lyklema, Colloids Surf., A **291**, 3 (2006).
[13] J. Lyklema, Adv. Colloid Interface Sci. **205**, 147 (2009).
[14] K. Besteman, M. Zevenbergen, H. Heering, and S. Lemay, Phys. Rev. Lett. **93**, 170802 (2004).
[15] K. Besteman, M. Zevenbergen, and S. Lemay, Phys. Rev. E **72**, 061501 (2005).
[16] F. H. J. Van Der Heyden, D. Stein, K. Besteman, S. G. Lemay, and C. Dekker, Phys. Rev. Lett. **96**, 224502 (2006).
[17] X. Wang, S. P. Devaiah, W. Zhang, and R. Welti, Prog. Lipid Res. **45**, 250 (2006).
[18] S. McLaughlin and D. Murray, Nature (London) **438**, 605 (2005).
[19] G. Di Paolo and P. De Camilli, Nature (London) **443**, 651 (2006).
[20] A. Travesset and D. Vaknin, EPL **74**, 181 (2006).
[21] C. Labbez, B. Jonsson, M. Skarba, and M. Borkovec, Langmuir **25**, 7209 (2009).
[22] A. Martin-Molina, J. A. Maroto-Centeno, R. Hidalgo-Alvarez, and M. Quesada-Perez, Colloids Surf., A **319**, 103 (2008).
[23] R. Israels, F. A. M. Leermakers, G. J. Fleer, and E. B. Zhulina, Macromolecules **27**, 3249 (1994).
[24] R. Nap, P. Gong and I. Szleifer, J. Polym. Sci., Part B: Polym. Phys. **44**, 2638 (2006).
[25] P. Gong, J. Genzer, and I. Szleifer, Macromolecules **40**, 8765 (2007).
[26] O. Hehmeyer, G. Arya, A. Z. Panagiotopoulos, and I. Szleifer, J. Chem. Phys. **126**, 244902 (2007).
[27] A. P. Nelson and D. A. McQuarrie, J. Theor. Biol. **55**, 13 (1975).
[28] A. Winiski, A. C. McLaughlin, R. V. McDaniel, M. Eisenberg, and S. McLaughlin, Biochemistry **25**, 8206 (1986).
[29] A. G. Moreira and R. R. Netz, EPL **57**, 911 (2002).
[30] D. B. Lukatsky and S. A. Safran, EPL **60**, 629 (2002).
[31] M. L. Henle, C. D. Santangelo, D. M. Patel, and P. Pincus, EPL **66**, 284 (2004).
[32] A. Travesset, Eur. Phys. J. E **17**, 435 (2005).
[33] J. Faraudo and A. Travesset, J. Phys. Chem. C **111**, 987 (2007).
[34] S. Madurga, A. Martín-Molina, E. Vilaseca, F. Mas, and M. Quesada-Pérez, J. Chem. Phys. **126**, 234703 (2007).
[35] H. Totsuji, Phys. Rev. A **17**, 399 (1978).
[36] S. McLaughlin, N. Mulrine, T. Gresalfi, G. Vaio, and A. McLaughlin, J. Gen. Physiol. **77**, 445 (1981).
[37] F. C. Tsui, D. M. Ojcius, and W. L. Hubbell, Biophys. J. **49**, 459 (1986).
[38] J. M. Bloch and W. Yun, Phys. Rev. A **41**, 844 (1990).
[39] D. Huster, K. Arnold, and K. Gawrisch, Biophys. J. **78**, 3011 (2000).
[40] I. Levental, P. Janmey, and A. Cebers, Biophys. J. **95**, 1199 (2008).
[41] S. Pandit and M. Berkowitz, Biophys. J. **82**, 1818 (2002).
[42] M. Yi, H. Nymeyer, and H.-X. Zhou, Phys. Rev. Lett. **101**, 038103 (2008).
[43] J. Faraudo and A. Travesset, Biophys. J. **92**, 2806 (2007).
[44] D. Vaknin, P. Krüger, and M. Lösche, Phys. Rev. Lett. **90**, 178102 (2003).
[45] J. Pittler, W. Bu, D. Vaknin, A. Travesset, D. J. McGillivray, and M. Lösche, Phys. Rev. Lett. **97**, 046102 (2006).
[46] W. Bu, K. Flores, J. Pleasants, and D. Vaknin, Langmuir **25**, 1068 (2009).
[47] S. Seok, T. J. Kim, S. Y. Hwang, Y. D. Kim, D. Vaknin, and D. Kim, Langmuir **25**, 9262 (2009).
[48] A. E. Martell and R. M. Smith, *Critical Stability Constants* (Plenum, New York, 1977), Vols. 2-3.
[49] R. A. Robinson and R. H. Stokes, *Electrolyte Solutions* (Dover, New York, 1959).
[50] S. Loverde and M. Olvera de la Cruz, J. Chem. Phys. **127**, 164707 (2007).
[51] A. Grzybowski, E. Gwozdz, and A. Brodka, Phys. Rev. B **61**, 6706 (2000).
[52] C. Calero and J. Faraudo, "Interaction between electrolyte and surfaces decorated with charged groups: A MD simulation study," J. Chem. Phys. (submitted).
[53] Y. Levin and M. Fisher, Physica A **225**, 164 (1996).
[54] S. Pianegonda, M. Barbosa, and Y. Levin, EPL **71**, 831 (2005).